

Supplemental Information

Reagents and chemicals

In the experiments, the related reagents are analytical reagents and can be used without further purification, which are described as follows: acetone (CH_3COCH_3 , Tianjin, FengChuan, 99.7%), isopropanol ($(\text{CH}_3)_2\text{CHOH}$, Tianjin, FengChuan, 99.7%), absolute ethanol ($\text{CH}_3\text{CH}_2\text{OH}$, Tianjin, FengChuan, 99.7%), zinc chloride hexahydrate ($\text{ZnCl}_2 \cdot 6\text{H}_2\text{O}$, Tianjin, GuangFu, 99%), cupric chloride dihydrate ($\text{CuCl}_2 \cdot 2\text{H}_2\text{O}$, Tianjin, GuangFu, 99%), indium chloride tetrahydrate ($\text{InCl}_3 \cdot 4\text{H}_2\text{O}$, Tianjin, GuangFu, 99%), Thioacetamide (CH_3CSNH_2 , Tianjin, GuangFu, 99%), absolute ethanol ($\text{C}_2\text{H}_6\text{O}$, Tianjin, GuangFu, 99.8%) sodium sulfate (Na_2SO_4 , Tianjin, GuangFu, 99%). The specifications of fluorine-doped tin oxide (FTO) glass are described as follows: The manufacturer is South China Science and Technology Ltd. The production size and experimental size are $10\text{ cm} \times 10\text{ cm} \times 0.22\text{ cm}$ and $1\text{ cm} \times 1\text{ cm} \times 0.22\text{ cm}$, respectively. The square resistance is less than $7\ \Omega$. The film thickness is 500 nm. The transmittance is more than 80%.

Preparation of n-type ZnIn_2S_4 and p-type CuInS_2

The n-type ZnIn_2S_4 nanosheets were prepared on fluorine-doped tin oxide (FTO) substrate through hydrothermal method, and the precursor solution is composed of 0.01 M Zinc chloride (ZnCl_2), 0.02 M Indium chloride tetrahydrate ($\text{InCl}_3 \cdot 4\text{H}_2\text{O}$) and 0.08 M Thioacetamide (CH_3CSNH_2). Subsequently, the solution was poured into the prepared Teflon-lined stainless steel and heated at $160\text{ }^\circ\text{C}$ for 12 h. The p-type CuInS_2 nanosheets were fabricated via alcohothermal method, 0.04 M $\text{CuCl}_2 \cdot 2\text{H}_2\text{O}$, 0.08 M $\text{InCl}_3 \cdot 4\text{H}_2\text{O}$ and 0.08 M CH_3CSNH_2 were dissolved in 12 mL absolute ethanol, stirring for 30 min to obtain precursor solution, which was poured into the Teflon lined stainless steel autoclave with FTO for 16 h at $180\text{ }^\circ\text{C}$.

Preparation of $\text{ZnIn}_2\text{S}_4/\text{CuInS}_2$ and $\text{CuInS}_2/\text{ZnIn}_2\text{S}_4$ photoelectrodes

Typically, the obtained $\text{ZnIn}_2\text{S}_4/\text{FTO}$ substrate is placed in a Teflon lined stainless steel autoclave and the $\text{ZnIn}_2\text{S}_4/\text{CuInS}_2$ heterojunction is prepared by the alcohothermal method as with the preparation of pure CuInS_2 . Similarly, the as-obtained $\text{CuInS}_2/\text{FTO}$ substrate is placed in a Teflon lined stainless steel autoclave with the conductive surface facing down at an angle of 45° , and the $\text{CuInS}_2/\text{ZnIn}_2\text{S}_4$ heterojunction was prepared by the hydrothermal method as with the preparation of pure ZnIn_2S_4 .

Characterization

The crystalline structures of samples were characterized by the data from X-ray diffractometer (XRD, Rigaku-D/max-2500; Cu $\text{K}\alpha$ radiation; $\lambda = 0.154059\text{ nm}$; working

voltage with 40 kV and working current with 150 mA). The morphology and microstructure of samples were carried out on Scanning electron microscopy (SEM, JEOL JSM-7800F) and JEOL JEM-2100 transmission electron microscopy (TEM). Incidentally, energy dispersive spectro-meter (EDS, AZtec from Oxford) element mapping was conducted to analyze the chemical composition and stoichiometry of obtained samples. The optical absorption performance of samples was examined via a DU-8B UV-Vis double-beam spectrophotometer (UV-visible absorption spectrometer). A series of PEC performances of the as-prepared samples were probed using a three-electrode device with the prepared films as working electrode, a platinum electrode as counter electrode and Ag/AgCl (saturated KCl) as reference electrode in 0.2 M Na₂SO₄ (pH=6.8) aqueous solution via an electrochemical workstation and irradiated with a Xenon lamp (AM 1.5 G, 100 mW·cm⁻²). The collected Ag/AgCl potential values were converted to the reversible hydrogen electrode (RHE) potential via using the equation: $E_{RHE} = E_{Ag/AgCl} + 0.059pH + 0.1976 \text{ V}$. A 300 W Xenon lamp was used to generate simulated sun light irradiation (AM 1.5 G, 100 mW/cm²). The electrochemical impedance spectra (EIS) measurements were collected on a three-electrode configuration with AC amplitude of 5 mV and frequency range of 10-100 kHz. Moreover, the surface photovoltage (SPV) measurements can characterization of the separation of photoinduced charge in photoelectrodes through the surface photovoltage spectrometer (PL-SPS/IPCE1000) indirectly. More importantly, the band energy level of ZnIn₂S₄ and CuInS₂ can be calculated via Ultraviolet photoelectron spectroscopy (UPS). the calculation was according to the following equations:

$$VBM = h\nu - (E_{cutoff} - E_{onset})$$

Where VBM is valence band maximum, $h\nu$ (nonmonochromatized He-I α radiation, $h\nu = 21.22 \text{ eV}$), the E_{cutoff} and E_{onset} is the secondary electron cut-off and binding energy onset, respectively.

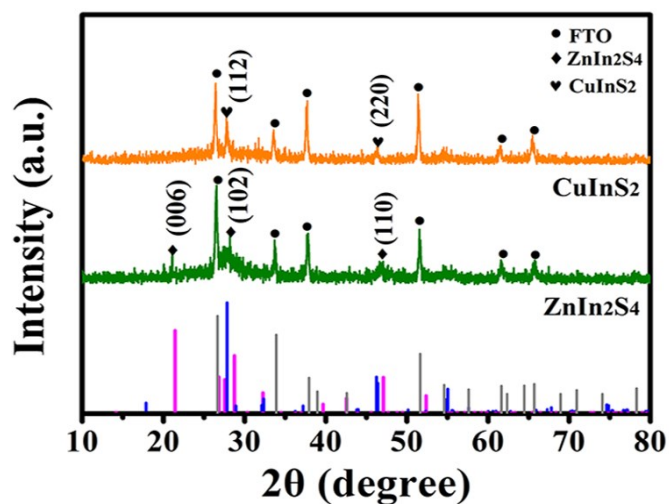


Fig. S1 XRD pattern of ZnIn₂S₄ and CuInS₂. The bottom peaks are standard position of ZnIn₂S₄ (JCPDS 72-0773, pink solid), CuInS₂ (JCPDS 82-1702, blue solid) and SnO₂ (JCPDS 77-0452, black solid)

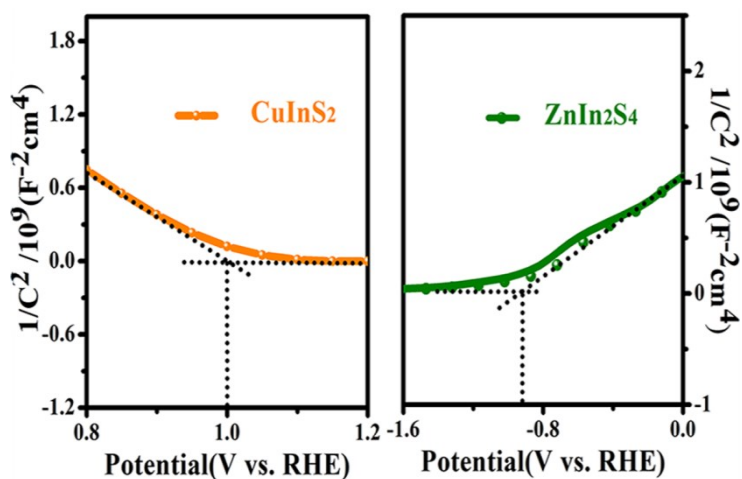


Fig. S2 Mott-Schottky plots of ZnIn₂S₄ and CuInS₂

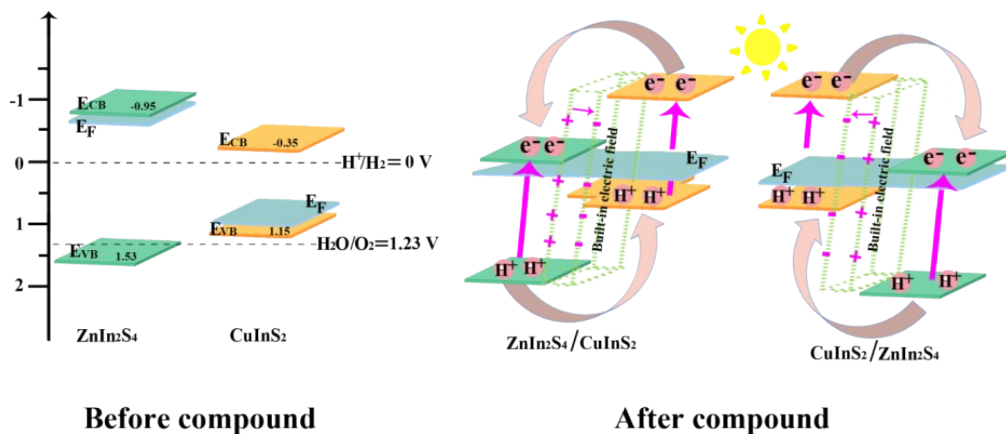


Fig. S3 Schematic diagram of ZnIn_2S_4 and CuInS_2 before and after forming bidirectional p-n heterojunction ($\text{ZnIn}_2\text{S}_4/\text{CuInS}_2$ p-n heterojunction and $\text{CuInS}_2/\text{ZnIn}_2\text{S}_4$ p-n heterojunction)

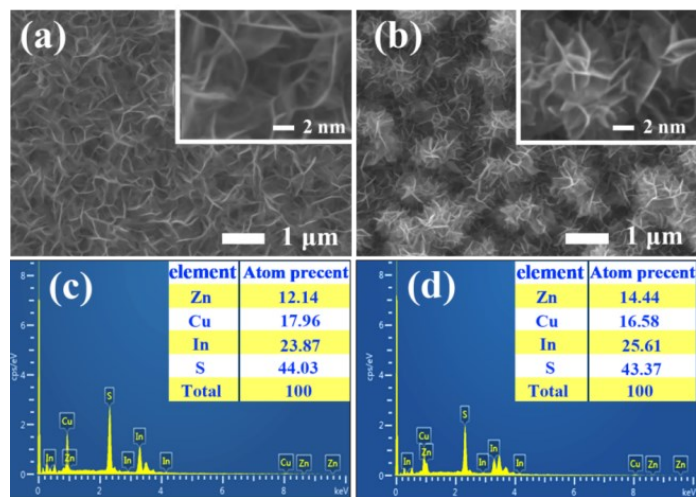


Fig. S4 The SEM images of (a) $\text{ZnIn}_2\text{S}_4/\text{CuInS}_2$ p-n heterojunction and (b) $\text{CuInS}_2/\text{ZnIn}_2\text{S}_4$ p-n heterojunction, the EDS spectrum of (c) $\text{ZnIn}_2\text{S}_4/\text{CuInS}_2$ p-n heterojunction and (d) $\text{CuInS}_2/\text{ZnIn}_2\text{S}_4$ p-n heterojunction

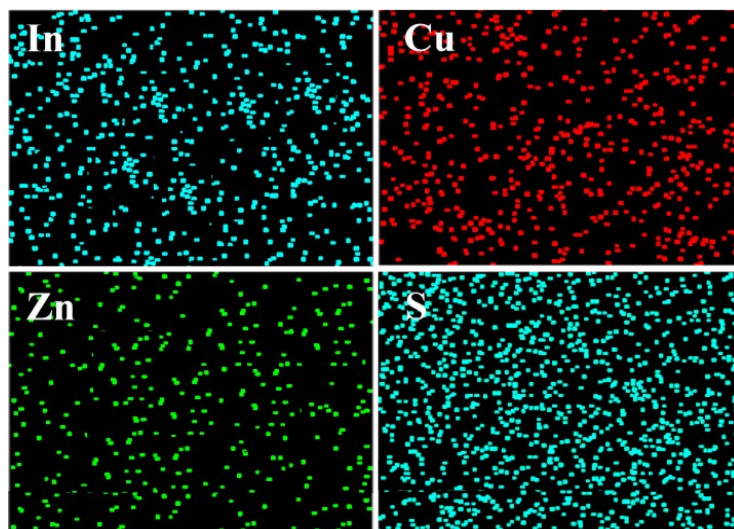


Fig. S5 Element distribution mapping

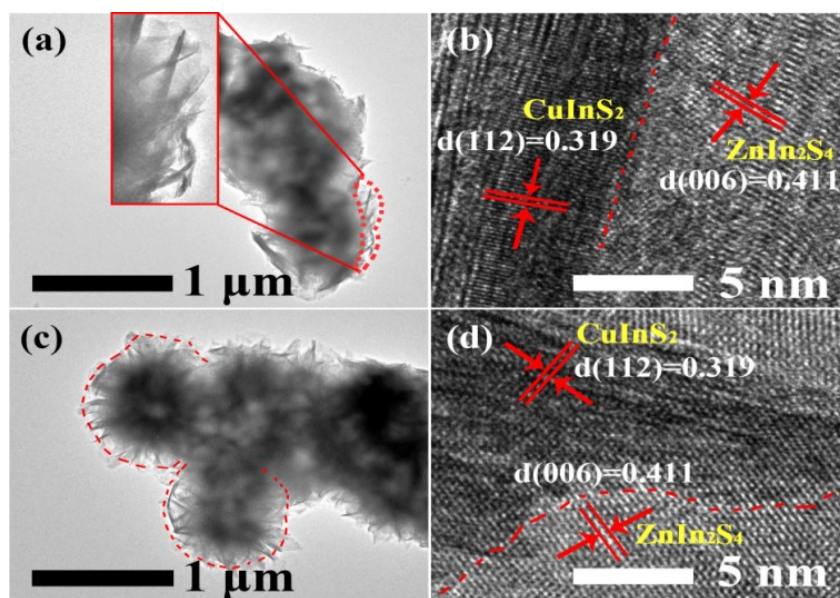


Fig. S6 TEM image (a) and HRTEM image (b) of ZnIn₂S₄/CuInS₂ p-n heterojunction, TEM image (c) and HRTEM image (d) of CuInS₂/ZnIn₂S₄ p-n heterojunction

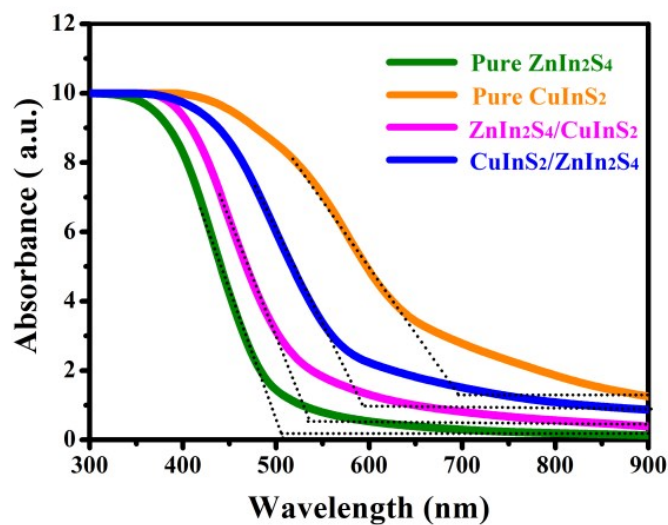


Fig. S7 UV-vis spectra of ZnIn₂S₄, CuInS₂, ZnIn₂S₄/CuInS₂ p-n heterojunction and CuInS₂/ZnIn₂S₄ p-n heterojunction

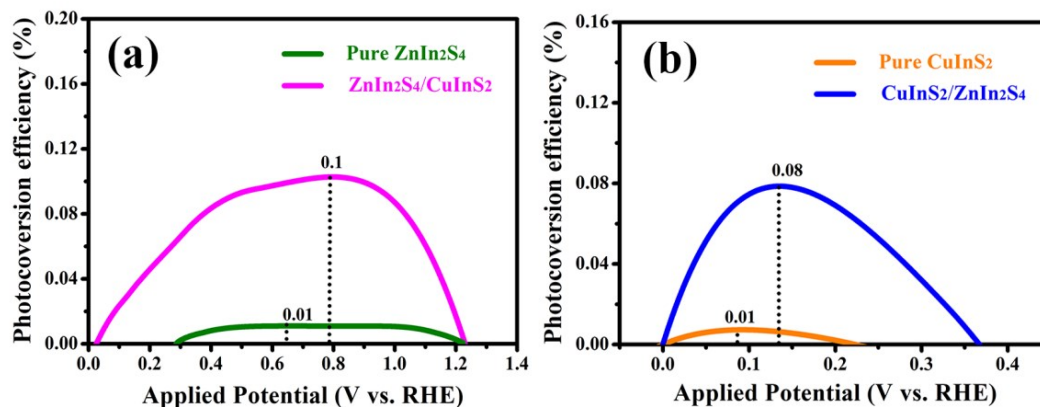


Fig. S8 Calculated applied bias photon-to-current efficiency (ABPE) curves of ZnIn₂S₄, CuInS₂, ZnIn₂S₄/CuInS₂ p-n heterojunction and CuInS₂/ZnIn₂S₄ p-n heterojunction

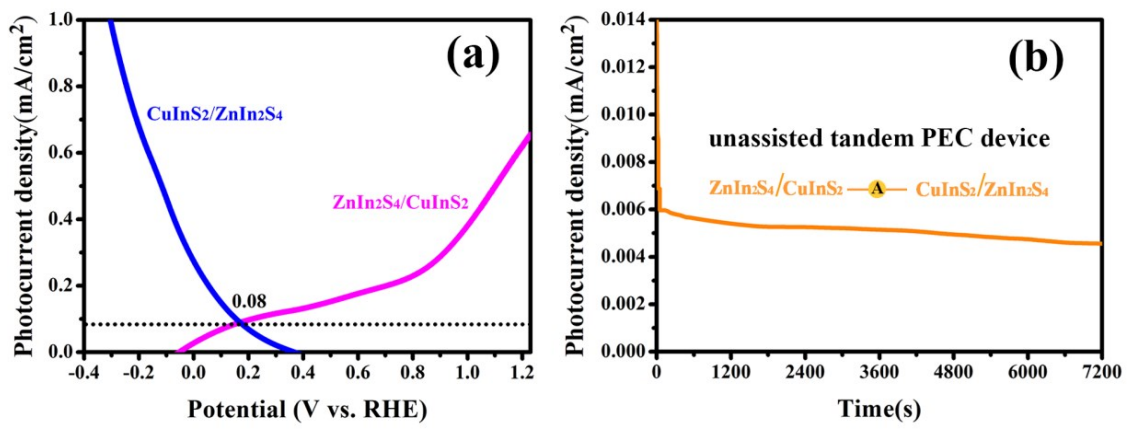


Fig. S9 (a) I–V curves of bidirectional p-n heterojunction photoelectrodes (ZnIn₂S₄/CuInS₂ photoanode and CuInS₂/ZnIn₂S₄ photocathode); (b) the I-T curve measured in unassisted tandem PEC cell device